Capture and release of quantum vortices using mechanical devices in low-temperature superfluids

Sanjay Shukla [1,*], Giorgio Krstulovic [2,†] and Rahul Pandit [1,‡]

[1]*Department of Physics, Centre for Condensed Matter Theory, Indian Institute of Science, Bangalore 560012, India*
[2]*Laboratoire Lagrange, Observatoire de la Côte d'Azur, CNRS, Universite Côte d'Azur, CS 34229 - F 06304 Nice, France*

We show that the Gross-Pitaevskii equation coupled with the wave equation for a wire (GP-W) provides a natural theoretical framework for understanding recent experiments employing a nanowire to detect a single quantum vortex in superfluid ^{4}He. We uncover the complete spatiotemporal evolution of such wire-based vortex detection via direct numerical simulations of the GP-W system. Furthermore, by computing the spatiotemporal spectrum, we obtain the vortex-capture-induced change in the oscillation frequency of the wire. We quantify this frequency shift by plotting the wire's oscillation frequency versus time and obtain results that closely match experimental observations. In addition, we provide analytical support for our numerical results by deriving the dispersion relation for the oscillating wire, with and without a trapped vortex. We show that the Magnus force opens a gap in the wire dispersion relation. The size of the gap becomes the characteristic frequency of the wire when a vortex is trapped.

Introduction. Vortex filaments are rapidly rotating thin localized structures in fluid flows. They play an important role in our understanding of such flows and their turbulence [1,2]. They appear as the dissipative structures of turbulent flow, and their dynamics has fascinated physicists and mathematicians for centuries [3]. Vortex filaments are also crucial in quantum fluids, such as superfluid helium and atomic BECs, as they are the most fundamental hydrodynamic excitation. Given their quantum origin, they are topological defects of the macroscopic wave function that describes the superfluid; the circulation of these defects assumes values that are multiples of the quantum of circulation $\mathcal{K} = h/m$, where h is the Planck constant and m the mass of the atoms.

The characterization and detection of such vortices is a challenge for condensed-matter science. The main difficulty is the vanishingly small core size, which is of the order of 1 Å in superfluid helium. Since the early experiments by Packard [4], experimentalists have made enormous progress in the detection of quantum vortices. Efforts to track and trap single quantum vortices have been made by groups that employ particles whose linear size is of the orders of micrometers, so it is considerably greater than the radius of the vortex core [5–7]. Such experiments have studied vortex reconnections [8] and Kelvin waves [9], and they have carried out a direct and accurate verification of Feynman's rule that relates the vortex density to the rotation rate [7].

Recently, a different experimental technique has been pioneered by Guthrie *et al.* [10], which has been successful in millikelvin superfluid ^{4}He for studiying signatures of the interaction, entrapment, and release of quantum vortices from nanobeams. These experiments rely on measurements of the frequency of the nanobeam and its modifications in time [10]. These changes in time have been interpreted as the trapping and release of a quantum vortex by the nanobeam; however, so far no theoretical or numerical support has been presented in support of this interpretation.

In this Letter, we design a model, based on the Gross-Pitaevskii equation (GPE), that is able to reproduce the results of the experiments of Guthrie *et al.* [10]. We show explicitly how the natural frequencies of a wire, immersed in the superfluid, are modified by the trapping and release of a quantum vortex. Figure 1 summarizes our results via flow visualizations and the evolution of the temporal spectra. We also provide a theory that explains the changes in wire frequencies when a vortex is trapped on it.

Our theoretical model uses the GPE to describe the superfluid via a complex macroscopic wave function ψ and a solid deformable thin cylindrical object, immersed in this superfluid, by an external potential. Our approach is similar to that used in the modeling of large particles in superfluids [11,12]. In particular, the cylinder is described by classical degrees of freedom and, for simplicity, we assume that the dynamics of the cylinder is given by the wave equation [13]. We refer to our model as the Gross-Pitaevskii-wire model (GP-W). The self-consistent coupled equations are derived by varying the total action of the system (see the Supplemental Material [14]). The GP-W system of equations is

$$i\hbar\frac{\partial\psi}{\partial t} = -\frac{\hbar^2}{2m}\nabla^2\psi + g|\psi|^2\psi - \mu\psi + V_{\text{ext}}(\mathbf{r} - \mathbf{R})\psi, \quad (1)$$

$$\ddot{\mathbf{q}} = -\frac{1}{\rho_w}\int dx\,dy V_w\nabla|\psi(x, y, \zeta)|^2 + c_w^2\frac{\partial^2\mathbf{q}}{\partial\zeta^2}, \quad (2)$$

where $\mathbf{r} = \{x, y, z\}$ is the three-dimensional (3D) spatial coordinate, $g > 0$ is the strength of the interaction between the

―――――
*Contact author: shuklasanjay771@gmail.com
†Contact author: giorgio.krstulovic@oca.eu
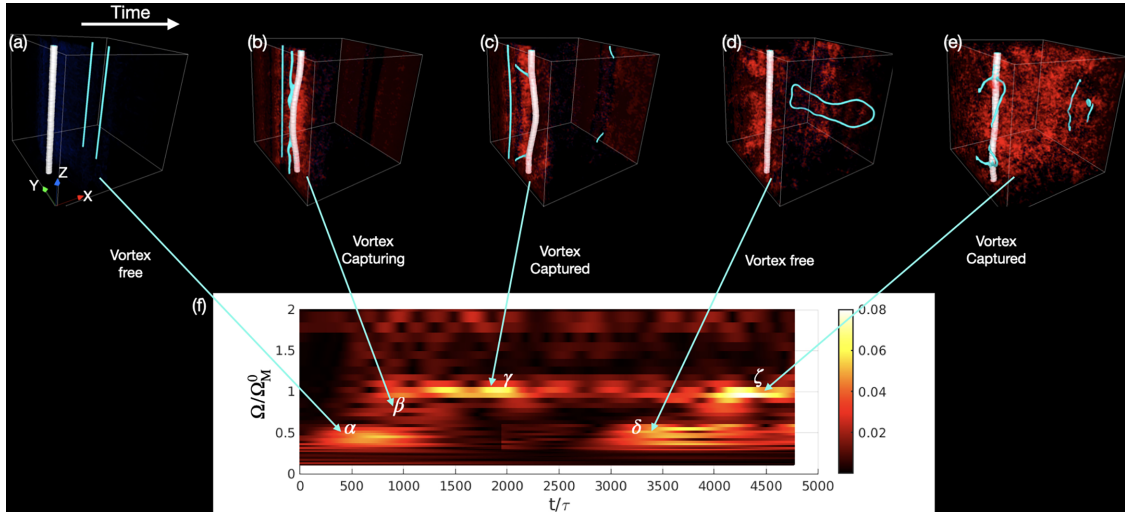‡Contact author: rahul@.iisc.ac.in

FIG. 1. Isosurface plots of the density $|\psi|^2$ showing the spatiotemporal evolution of two quantum vortices (in cyan) interacting with the oscillating wire (in gray), which is depicted via the isosurface of the wire's potential V_w, in our GP-W model (see text), at five representative times that increase from left to right: (a) a vortex-free state labeled by α; (b) a vortex-capturing state β; (c) a vortex-captured state γ; (d) a vortex-disentangled state δ; and (e) a vortex-recaptured state ζ. These isosurface plots are superimposed on volume plots of $|\psi|^2$, in which sound waves appear as red clouds. (f) Filled contour plot of the absolute value of the continuous wavelet transform (CWT), which we obtain via the windowed Fourier transform in MATLAB, of the wire's position $\mathbf{q} = (q_x, q_y)$ as a function of the normalized frequency Ω/Ω_M^0 of the wire and time t/τ. The noteworthy changes in Ω/Ω_M^0 are associated with the configurations in (a)–(e) are labeled α, β, γ, δ, and ζ, respectively.

bosons, μ the chemical potential, and V_w the potential that accounts for the wire, whose centerline is parametrized by $\mathbf{R}(\zeta) \equiv \{q_x(\zeta), q_y(\zeta), \zeta\}$, where ζ is the parameter that varies along the central axis of the wire. Equation (2) governs the dynamics of the wire, with $\mathbf{q} \equiv (q_x, q_y)$ the transverse displacement of the wire of density per unit length ρ_w, and speed of sound c_w. Specifically, Eq. (2) describes a vibrating string with the linear dispersion relation. We model the wire by a Gaussian potential

$$V_{\text{ext}}(\mathbf{r} - \mathbf{R}) = \lim_{\epsilon \to 0} \int V_w \frac{e^{-\frac{(z-\zeta)^2}{2\epsilon^2}}}{\sqrt{2\pi \epsilon^2}} d\zeta, \qquad (3)$$

with

$$V_w = V_0 \exp\left(-\frac{[x - q_x(\zeta)]^2 + [y - q_y(\zeta)]^2}{2a^2}\right), \qquad (4)$$

where V_0 and a are, respectively, its strength and width. In Eq. (3), the Gaussian function along the z direction, which becomes the delta function as its width $\epsilon \to 0$, is used to derive Eq. (2) from the Hamiltonian (see the Supplemental Material [14]). The GP-W system conserves the number of particles $N = \int |\psi|^2 d\mathbf{r}$, the total energy E, and the total momentum $\mathbf{P}$ (see the Supplemental Material [14]).

The wire, with mass M_w^0, length L_w, and radius a_w, displaces some superfluid, whose (added) mass is $M_w = m \int (|\psi_\infty|^2 - |\psi_w|^2) d\mathbf{r}$, where ψ_∞ and ψ_w are, respectively, the steady-state wave functions without and with the wire. The radius of the wire is calculated using the displaced mass as $a_w = (\frac{3M_w}{\rho 4\pi})^{1/3}$, where $\rho \sim |\psi_\infty|^2$. The mass ratio and effective mass

$$\mathcal{M} \equiv \frac{M_w^0}{M_w} \quad \text{and} \quad M_w^{\text{eff}} = M_w^0 + M_w \qquad (5)$$

help us to distinguish between light ($\mathcal{M} < 1$) and heavy ($\mathcal{M} > 1$) wires. The frequency of the wire, when a vortex is trapped on it, is obtained by a balance of its inertia and the Magnus force [15] and is

$$\Omega_M^0 = \frac{\rho \Gamma L_w}{M_w^{\text{eff}}}, \qquad (6)$$

where $\Gamma = n_v h/m$ is the quantized circulation with n_v being the multiplicity of the vortex and ρ is the superfluid density.

Models of the type (1) and (2) account naturally for the processes of vortex trapping and release by solid boundaries, without recourse to any *ad hoc* rule, so they have been used with great success, numerically and theoretically, to study the dynamics of particles in superfluids [11], the interaction of particles and quantum vortices [12,15,16], vortex reconnections with trapped particles [17], and active Lagrangian superfluid turbulence [18]. The GPE is derived for weakly interacting Bose-Einstein condensates (BECs). Even though ^{4}He is a strongly interacting system, GPE-type models reproduce its observed hydrodynamical behavior well, at least qualitatively. Therefore, our GP-W model provides a powerful framework for the development of a theoretical understanding of the experiments [10] that use nanomechanical devices to study vortex dynamics in superfluid ^{4}He.

To study Eqs. (1)–(4), we perform direct numerical simulations (DNSs) via a Fourier pseudospectral method on a periodic cubical domain of side $L = 2\pi$, with $N^3 = 256^3$ or $N^3 = 512^3$ collocation points, and the 2/3 rule for dealiasing [19–21], i.e., spectral truncation of Fourier modes for wave numbers $k = |\mathbf{k}| > k_{\max} = N/3$. In our DNSs, lengths are normalized by the healing length ξ and time by $\tau = \xi/c_s$. We set the speed of sound to be $c_s = 1$; and the healing length is $\xi = 2dx$, where $dx = L/N$. For time marching, we use the fourth-order Runge-Kutta scheme RK4 for Eq. (1)

and the exponential time differencing RK4 scheme [22] for Eq. (2), because the ratio c_w/c_s is large. In our study, the radius and the length of the wire are, respectively, $a_w \simeq 3\xi$ and $L_w \simeq 256\xi$; the corresponding numbers in the nanobeam experiments [10] with ^{4}He are $a_w \simeq 100\xi$ and $L_w \simeq 10^4\xi$. Thus, the ratio a_w/L_w in our DNSs is comparable to that in experiments, so our study should be able to capture the essential properties of the wire-vortex interactions that have been observed in these experiments [10].

We use an initial condition ψ_{vw} (see the Supplemental Material [14] and Ref. [23] therein), in which a vortex-antivortex pair is positioned away from the wire; furthermore, we include a small perturbation on **q**. As time t progresses, the wire oscillates, the vortex-antivortex pair moves towards the wire, one of them gets captured by it, whereupon the frequency of the wire changes. An illustrative sequence of vortex capture, disentanglement, and recapture events is shown via pseudo-color plots in Figs. 1(a)–1(e). In Fig. 1(f), we show a filled contour plot of the absolute value of the continuous wavelet transform (CWT) of the wire's position $\mathbf{q} = (q_x, q_y)$ as a function of the normalized frequency Ω/Ω_M^0 of the wire and time t/τ. Note the changes in Ω/Ω_M^0 that are associated with the configurations in Figs. 1(a)–1(e) that are labeled α, β, γ, δ, and ζ, respectively. Clearly, our DNS reproduces the observed experimental behaviors of the nanobeam in Ref. [10], and it confirms that the changes in Ω/Ω_M^0 arise from vortex trapping or disentangling. Furthermore, we observe the frequency of the wire, when the vortex is trapped on it, corresponds to the one given by the Magnus force (6). It is also important to note that, when the vortex is not trapped, the frequency of the wire is $\simeq 0.4\Omega_M^0$, which depends on the initial perturbation around the mean position of the wire and corresponds to the frequency of the dominant mode of vibration.

We now develop a theory that allows us to understand the modification of the wire's natural frequency because of its interaction with the vortex.

In the absence of quantized vortices and with $V_w = 0$, we can linearize the GPE in Eq. (1) about the uniform equilibrium state $|\psi|^2 = n_0$ to obtain the Bogoliubov dispersion [24] relation

$$\Omega_B(k) = c_s |\mathbf{k}| \left(1 + \tfrac{1}{2}\xi^2 |\mathbf{k}|^2 \right)^{1/2}, \qquad (7)$$

where $c_s = \sqrt{gn_0/m}$ is the speed of sound, $\mathbf{k}$ is the wave vector of the excitation, and the healing length $\xi = \hbar/\sqrt{2gmn_0}$, which yields the vortex-core radius. Fluctuations of quantum vortices include Kelvin waves (KWs). The frequency spectrum Ω_{KW} for Kelvin waves was derived by Kelvin for a hollow vortex in an incompressible Euler fluid [3],

$$\Omega_{KW}(k) = \frac{\Gamma}{2\pi a_0^2}\left[1 - \sqrt{1 + a_0 k \frac{K_0(a_0 k)}{K_1(a_0 k)}} \right], \qquad (8)$$

where $K_n(x)$ is the order-n modified Bessel function and k is the magnitude of the wave vector. Roberts [25] showed that the dispersion relation in Eq. (8) is also valid for a quantum vortex in GPE at small wave numbers and obtained $a_0 \simeq 1.1265\xi$. Because of the lack of a full analytical dispersion relation of vortex excitations in the GPE, we use the

following fit to the dispersion relation in our simulations [15],

$$\Omega_v^{\text{fit}} = \Omega_{KW}\left[1 + \epsilon_{\frac{1}{2}}(a_0 k)^{\frac{1}{2}} + \epsilon_1(a_0 k) + \tfrac{1}{2}(a_0 k)^{\frac{3}{2}} \right], \qquad (9)$$

where $\epsilon_{\frac{1}{2}} = -0.20$ and $\epsilon_1 = 0.64$ are dimensionless parameters. For a small wave number, $\Omega_v^{\text{fit}} \to \Omega_{KW}$, while for a large wave number, $\Omega_v^{\text{fit}} \propto k^2$, which is a free-particle dispersion relation, applicable for small-scale excitations of a superfluid vortex.

If we consider the wire in the superfluid without vortices, then, in the long-wavelength limit, the dispersion relation for the wire frequency is [26]

$$\Omega_w^{\pm}(k) \sim \pm c_w k \left(\frac{1}{1 + \frac{1}{\mathcal{M}}} \right)^{1/2}, \quad k \to 0, \qquad (10)$$

where c_w is the speed of sound in the wire and the effect of the superfluid appears via $\mathcal{M}$, which accounts for the added mass [Eq. (5)]. The dispersion relation in Eq. (10) is the solution of Eq. (2) in the long-wavelength limit. In the following, we verify it using our DNS of the GP-W model. To study the wire's dispersion in Eq. (10) without a vortex, we use an initial condition ψ_w (see the Supplemental Material [14]) in which all the modes of the wire are excited with a small amplitude such that the amplitude is inversely proportional to the wave number k. So, the lowest mode is excited with the highest amplitude (see the Supplemental Material [14]). In our DNS for the GP-W model, we obtain the spatiotemporal spectrum $S_q(k, \omega) \sim |q(k, \omega)|^2$, where q is the magnitude of the displacement of the wire [see Eq. (2)]. In Fig. 2(a) we show a representative plot of the wire (in gray) superimposed on a volume plot of $|\psi|^2$, whose fluctuations indicate sound waves. The dispersion relation (10) is in good agreement with the low-k part of high-intensity regions in the filled contour plot of $S_q(k, \omega)$ [Figs. 2(b) and 2(c) for two values of $\mathcal{M} = 2$ and $\mathcal{M} = 5$]; these high-intensity regions yield the complete dispersion relation for all values of k.

To study how the wire's dispersion relation changes when a vortex is trapped on it, we use an initial condition with a perturbed wire enrobed by a vortex (see Supplemental Material [14]). For convenience, we chose $\Gamma < 0$, so that Kelvin-wave excitations lie in the upper part of the dispersion relation. The measured dispersion relation for this system is presented in Fig. 3(b). Remarkably, the vortex modifies the excitation spectrum of the wire; in particular, it lifts the degeneracy, at $k = 0$, as is apparent in Fig. 3(c). We chose a different set of parameters in Fig. 3(b) as compared to that in Fig. 2(b) so that the gap in Fig. 3(b) is much more enhanced, leaving the physics unchanged. The measured dispersion relation matches with the analytical dispersion form in Eq. (13), which we derive in the following section.

To understand this perturbed spectrum, we derive an effective equation that governs the dynamics of the wire in the presence of a vortex. First, we write the wire displacement in complex form $q = q_x + iq_y$. Then, following the ideas of Ref. [15], a simple equation for q is obtained by balancing the Magnus force $i\Omega_M^0(\dot{q} - v_{\text{si}})$, the tension $c_w^2 \partial_{zz} q$, and wire inertia. Here, v_{si} is the self-induced velocity at position q, which depends on the model. For the sake of simplicity, we first employ the local-induction approximation (LIA) [27],
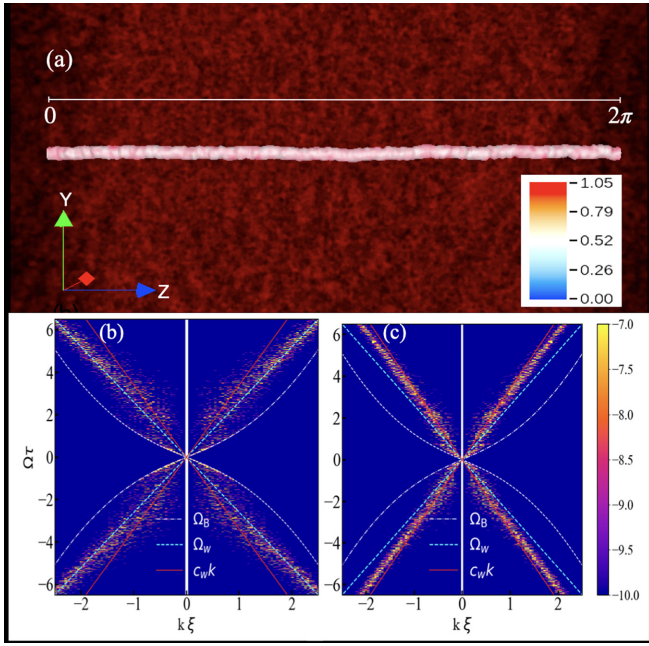
FIG. 2. (a) One level contour plot of wire immersed in GP-W system, showing small-amplitude oscillations; this is superimposed on a volume plot of $|\psi|^2$. (b) Filled contour plot of the spatiotemporal spectrum $S_q(k, \omega)$ (see text) of the wire on log scale; the cyan dashed line represents the linear dispersion relation of Eq. (10) with $\mathcal{M} = 2$, $c_s/c_w = 1/3.3$, and the radius of the wire $a_w = 2.50\xi$. The white dashed line shows the Bogoliubov dispersion curve of Eq. (7), and the sold red line shows the dispersion relation $c_w k$ without accounting for added mass effects. (c) is the same as (b) but for $\mathcal{M} = 5$ with other parameters fixed.

in which the superfluid flow velocity can be approximated by $v_{si} = i \frac{\Gamma}{4\pi} \Lambda \frac{\partial^2}{\partial z^2} \mathbf{R}(z, t)$, where Λ is a constant in this approximation of the order of $\log(\ell/\xi)$, with ℓ the intervortex distance. Note that in the LIA framework, Kelvin waves have the dispersion relation $\Omega_{\text{LIA}} = -\frac{\Gamma \Lambda k^2}{4\pi}$. The dynamics of the wire is governed by

$$\ddot{q}(z, t) = i\Omega_M^0 \left[\dot{q}(z, t) - i \frac{\Gamma}{4\pi} \Lambda \frac{\partial^2}{\partial z^2} q(z, t) \right] + c_w^2 \frac{\partial^2}{\partial z^2} q(z, t). \tag{11}$$

The previous equation is a natural generalization of the model introduced in Ref. [15].

We now seek solutions of Eq. (11) of the form $q(z, t) = q_0 e^{i(\Omega_M^\pm t - kz)}$ and then obtain their frequency

$$\Omega_M^\pm(k) = \frac{\Omega_M^0}{2} \pm \frac{1}{2} \sqrt{\left(\Omega_M^0\right)^2 + \left(\frac{\Omega_M^0 \Gamma \Lambda}{\pi} + 4c_w^2\right) k^2}. \tag{12}$$

We can go beyond the LIA by following Ref. [15] to obtain the following dispersion relation for the waves along the wire,

$$\Omega_M^\pm(k) = \frac{\Omega_M^0}{2} \pm \frac{1}{2} \sqrt{\left(\Omega_M^0\right)^2 - 4\Omega_M^0 \Omega_v + 4c_w^2 k^2}, \tag{13}$$

where Ω_v is a model-dependent bare vortex frequency. If we use the LIA, $\Omega_v = \Omega_{\text{LIA}}$, so Eq. (13) becomes Eq. (12); to go beyond the LIA we use $\Omega_v = \Omega_v^{\text{fit}}$, which is given by Eq. (9).
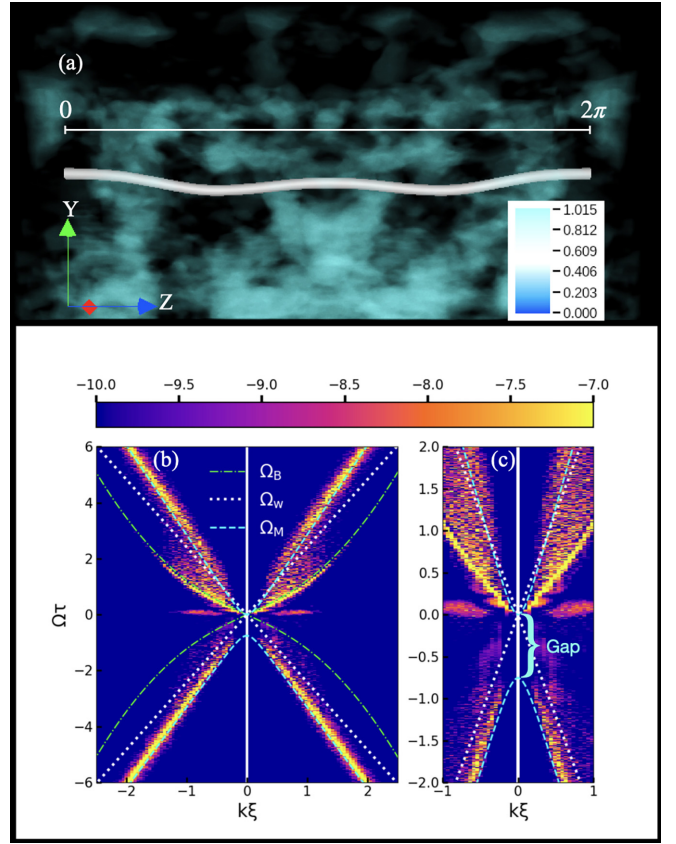

FIG. 3. One level contour plots depicting the wire in gray loaded with a vortex (a) at an intermediate time. The cyan cloud in (a) represents the sound waves, which is a volume plot of $|\psi|^2$. (b) The spatiotemporal spectrum $S_q(k, \omega) \sim |q(k, \omega)|^2$ of the wire on a log scale placed at the location of a bare vortex, featuring small-amplitude Kelvin waves. The white dashed curve represents the dispersion relation from Eq. (7), whereas the cyan dashed line corresponds to the analytical dispersion relation in Eq. (13). The green dotted-dashed line shows the Bogoliubov dispersion curve of Eq. (7). (c) A closer examination of (b) that focuses on the central region. Here, we have used $\mathcal{M} = 4.0$, $c_s/c_w = 1/2.7$, and the radius of the wire is $a_w = 1.84\xi$.

In the absence of a vortex, the wire's frequency spectrum (10) exhibits a gapless mode with $\Omega_w^\pm(k = 0) = 0$. This mode develops a gap, i.e., $\Omega_M^+(k = 0) - \Omega_M^-(k = 0) = \Omega_M^0 > 0$, when a vortex is introduced [see Eqs. (13) and Fig. 3(c)]. The gap observed in our GP-W simulations is well explained by our theoretical prediction. Furthermore, the whole dispersion relation is reproduce by our theory *without any adjustable parameter*, when we use the bare Kelvin-wave dispersion-relation fit Ω_v^{fit}.

Conclusions. Superfluid turbulence is often envisioned as a tangle of quantum vortices [28–35]. It is important, therefore, to detect such vortices unambiguously, which has been the goal of several experiments [4,5,7,8,10,36,37]. The use of wires or nanobeams [10,37] has led to very promising results that have shown how a vortex interacts with a wire. We have carried out a GPE study that has been designed to uncover such wire-vortex interactions and is therefore of direct relevance to the experiments of Refs. [10,37]. In particular, we have obtained various signatures of the capture of a superfluid

vortex by a wire using our DNS of the GP-W system. In the absence of any quantized vortices in the system, the wire oscillates with a frequency characterized by the initial random disturbance. We quantify how the wire-vortex interaction changes the oscillation frequency of the wire. In particular, we monitor the temporal evolution of the normalized frequency Ω/Ω_M^0 to identify (Fig. 1) of vortex-free, vortex-trapping, and vortex-trapped states as in the experiments of Ref. [10]. Our computation of the spatiotemporal spectrum allows us to obtain dispersion relations [Figs. 2(b) and 3(b)] without and with vortices on the wire. In particular, without a vortex, the transverse displacements of the wire, along two perpendicular directions, lead to a degeneracy in the excitation spectra (Figs. 2 and 3). If the vortex is present, a Magnus force acts on the wire because of the circulation of the vortex; this lifts the degeneracy in the frequency spectrum and leads to a gap. This Magnus force produces two circularly polarized modes that are separated by the frequency Ω_M^0. This frequency thus

becomes dominant for sufficiently large-scale perturbations, explaining the jumps observed on the inset of Fig. 3. We show that our DNS results are in good agreement with our simple linear theory. Finally, our model is easily generalizable to describe different types of mechanical devices, or the dynamics of several devices connected by vortices.

[1] A. J. Majda, A. L. Bertozzi, and A. Ogawa, Vorticity and incompressible flow. Cambridge texts in applied mathematics, Appl. Mech. Rev. **55**, B77 (2002).

[2] A. J. Chorin, *Vorticity and Turbulence* (Springer, Berlin, 2013), Vol. 103.

[3] W. Thomson, XXIV. Vibrations of a columnar vortex, London, Edinburgh Dublin Philos. Mag. J. Sci. **10**, 155 (1880).

[4] R. E. Packard and T. M. Sanders, Detection of single quantized vortex lines in rotating He II, Phys. Rev. Lett. **22**, 823 (1969).

[5] G. Bewley, D. Lathrop, and K. Sreenivasan, Visualization of quantized vortices, Nature (London) **441**, 588 (2006).

[6] M. L. Mantia and L. Skrbek, Quantum turbulence visualized by particle dynamics, Phys. Rev. B **90**, 014519 (2014).

[7] C. Peretti, J. Vessaire, É. Durozoy, and M. Gibert, Direct visualization of the quantum vortex lattice structure, oscillations, and destabilization in rotating ^{4}He, Sci. Adv. **9**, eadh2899 (2023).

[8] G. P. Bewley, M. S. Paoletti, K. R. Sreenivasan, and D. P. Lathrop, Characterization of reconnecting vortices in superfluid helium, Proc. Natl. Acad. Sci. USA **105**, 13707 (2008).

[9] E. Fonda, D. P. Meichle, N. T. Ouellette, S. Hormoz, and D. P. Lathrop, Direct observation of Kelvin waves excited by quantized vortex reconnection, Proc. Natl. Acad. Sci. USA **111**, 4707 (2014).

[10] A. Guthrie, S. Kafanov, M. T. Noble, Y. A. Pashkin, G. R. Pickett, V. Tsepelin, A. A. Dorofeev, V. A. Krupenin, and D. E. Presnov, Nanoscale real-time detection of quantum vortices at millikelvin temperatures, Nat. Commun. **12**, 2645 (2021).

[11] V. Shukla, R. Pandit, and M. Brachet, Particles and fields in superfluids: Insights from the two-dimensional Gross-Pitaevskii equation, Phys. Rev. A **97**, 013627 (2018).

[12] U. Giuriato and G. Krstulovic, Interaction between active particles and quantum vortices leading to Kelvin wave generation, Sci. Rep. **9**, 4839 (2018).

[13] More sophisticated mechanical models, such as for a rectangular beam, can be obtained by a straightforward generalization of our model.

[14] See Supplemental Material at http://link.aps.org/supplemental/10.1103/PhysRevB.111.L100504 for containing the following: (1) the Hamiltonian and total energy describing the Gross-Pitaevskii system with vibrating wire. (2) Details of the preparations of initial conditions for Figs. 1–3.

[15] U. Giuriato, G. Krstulovic, and S. Nazarenko, How trapped particles interact with and sample superfluid vortex excitations, Phys. Rev. Res. **2**, 023149 (2020).

[16] A. Griffin, V. Shukla, M.-E. Brachet, and S. Nazarenko, Magnus-force model for active particles trapped on superfluid vortices, Phys. Rev. A **101**, 053601 (2020).

[17] U. Giuriato and G. Krstulovic, Quantum vortex reconnections mediated by trapped particles, Phys. Rev. B **102**, 094508 (2020).

[18] U. Giuriato and G. Krstulovic, Active and finite-size particles in decaying quantum turbulence at low temperature, Phys. Rev. Fluids **5**, 054608 (2020).

[19] G. Krstulovic and M. Brachet, Energy cascade with small-scale thermalization, counterflow metastability, and anomalous velocity of vortex rings in Fourier-truncated Gross-Pitaevskii equation, Phys. Rev. E **83**, 066311 (2011).

[20] T. Y. Hou and R. Li, Computing nearly singular solutions using pseudo-spectral methods, J. Comput. Phys. **226**, 379 (2007).

[21] S. Shukla, A. K. Verma, M. E. Brachet, and R. Pandit, Gravity- and temperature-driven phase transitions in a model for collapsed axionic condensates, Phys. Rev. D **109**, 063009 (2024).

[22] S. M. Cox and P. C. Matthews, Exponential time differencing for stiff systems, J. Comput. Phys. **176**, 430 (2002).

[23] N. G. Berloff, Padé approximations of solitary wave solutions of the Gross–Pitaevskii equation, J. Phys. A: Math. Gen. **37**, 1617 (2004).

[24] N. Bogoliubov, On the theory of superfluidity, J. Phys. (USSR) **11**, 23 (1947).

[25] P. H. Roberts, On vortex waves in compressible fluids. II. The condensate vortex, Proc. R. Soc. Lond. A **459**, 597 (2003).

[26] A. L. Fetter and K. Harvey, Elastic filaments and vortex waves, Phys. Rev. A **4**, 2305 (1971).

[27] R. J. Arms and F. R. Hama, Localized-induction concept on a curved vortex and motion of an elliptic vortex ring, Phys. Fluids **8**, 553 (1965).

[28] R. Feynman, Application of quantum mechanics to liquid helium, Prog. Low Temp. Phys. **1**, 17 (1955).

[29] K. Schwarz, Generation of superfluid turbulence deduced from simple dynamical rules, Phys. Rev. Lett. **49**, 283 (1982).

[30] R. J. Donnelly, Superfluid turbulence, Sci. Am. **259**, 100 (1988).

[31] L. Skrbek and K. R. Sreenivasan, Developed quantum turbulence and its decay, Phys. Fluids **24**, 011301 (2012).

[32] C. F. Barenghi, L. Skrbek, and K. R. Sreenivasan, Introduction to quantum turbulence, Proc. Natl. Acad. Sci. USA **111**, 4647 (2014).

[33] L. Skrbek, D. Schmoranzer, Š. Midlik, and K. R. Sreenivasan, Phenomenology of quantum turbulence in superfluid helium, Proc. Natl. Acad. Sci. USA **118**, e2018406118 (2021).

[34] M. S. Paoletti and D. P. Lathrop, Quantum turbulence, Annu. Rev. Condens. Matter Phys. **2**, 213 (2011).

[35] C. F. Barenghi, L. Skrbek, and K. R. Sreenivasan, *Quantum Turbulence* (Cambridge University Press, Cambridge, UK, 2023).

[36] Y. Minowa, S. Aoyagi, S. Inui, T. Nakagawa, G. Asaka, M. Tsubota, and M. Ashida, Visualization of quantized vortex reconnection enabled by laser ablation, Sci. Adv. **8**, eabn1143 (2022).

[37] Y. Nago, A. Nishijima, H. Kubo, T. Ogawa, K. Obara, H. Yano, O. Ishikawa, and T. Hata, Vortex emission from quantum turbulence in superfluid ^{4}He, Phys. Rev. B **87**, 024511 (2013).